

CORRELATIONS BETWEEN CENTRAL MASSIVE OBJECTS AND THEIR HOST GALAXIES: FROM BULGELESS SPIRALS TO ELLIPTICALS

YUEXING LI¹, ZOLTÁN HAIMAN², MORDECAI-MARK MAC LOW³

¹Institute for Theory and Computation, Harvard-Smithsonian Center for Astrophysics, Harvard University, 60 Garden Street, Cambridge, MA 02138

²Department of Astronomy, Columbia University, New York, NY 10027 and

³Department of Astrophysics, American Museum of Natural History, 79th Street at Central Park West, New York, NY 10024

Accepted to ApJ

ABSTRACT

Recent observations reveal that a majority of galaxies contain a central massive object (CMO), either a supermassive black hole (SMBH) or a compact stellar nucleus, regardless of the galaxy mass or morphological type. The masses of these CMOs correlate tightly with those of the host galaxies, $M_{\text{CMO}} \approx 0.002 M_{\text{gal}}$. Several recent studies argue that feedback from black holes can successfully explain the $M_{\text{BH}}-\sigma$ correlation in massive elliptical galaxies that contain SMBHs. However, puzzles remain in spirals or dwarf spheroids that do not appear to have black holes but instead harbor a compact central stellar cluster. Here we use three-dimensional, smoothed particle hydrodynamics simulations of isolated galaxies to study the formation and evolution of CMOs in bulgeless disk galaxies, and simulations of merging galaxies to study the transition of the CMO-host mass relation from late-type bulgeless spirals to early-type ellipticals. In the simulations, absorbing sink particles represent either SMBHs or star clusters, while stellar feedback on the gas is implemented by assuming an isothermal equation of state with effective sound speed of order 10 km s^{-1} . Our simulations show that the mass of the CMO correlates with that of the host galaxy in both isolated bulgeless spirals and in ellipticals formed through mergers, and that M_{CMO} correlates with the global star-formation efficiency in the galaxy. We find that the final mass of the CMO is dominated by the accreted mass, rather than the initial fragment mass. The denser nuclei of more massive galaxies have higher mass accretion rates, and both the final accreted CMO mass and the recently formed stellar mass increase monotonically with the total mass of the galaxy. Our results suggest that the observed correlations may be established primarily by the depletion of gas in the central region by accretion and star-formation, and may hold for all galaxy types. A systematic search for CMOs in the nuclei of bulgeless disk galaxies would offer a test of this conclusion.

Subject headings: galaxy: nuclei — galaxy: spirals — galaxy: ellipticals — galaxy: evolution — galaxy: kinematics and dynamics — galaxy: ISM — galaxy: star clusters — stars: formation

1. INTRODUCTION

Supermassive black holes (SMBHs) appear to exist in most, if not all, galaxies (see, e.g., the reviews by Haiman & Quataert 2004 and Ferrarese & Ford 2005). Over the past few years, SMBHs have been detected in about 40 nearby galaxies using gas and stellar dynamical methods (e.g., Kormendy & Richstone 1995; Richstone et al. 1998; Ho 1999; Merritt & Ferrarese 2001). These galaxies include nearby ellipticals and lenticulars (e.g., Marconi et al. 1997; Macchetto et al. 1997), as well as spirals with bulges such as the Milky Way (Genzel et al. 1997; Ghez et al. 2000, 2003; Schödel et al. 2002). Most of these galaxies are luminous ones with total masses larger than $10^{12} M_{\odot}$. There appear to be tight correlations between the masses of the SMBHs, M_{BH} , and the global properties of the spheroid components of their hosts, such as their luminosities and masses (Magorrian et al. 1998; Marconi & Hunt 2003), light concentration (Graham et al. 2001), and velocity dispersions (Ferrarese & Merritt 2000; Gebhardt et al. 2000; Tremaine et al. 2002).

Recently, low- and intermediate-luminosity galaxies, with $M_{\text{B}} \gtrsim -18$ mag, have been studied by Wehner & Harris (2006) using the Hubble Space Telescope (HST) Wide-Field/Planetary Camera Dwarf Elliptical Galaxy Snapshot Survey of the Leo Group and Virgo and Fornax clusters

(Lotz, Miller, & Ferguson 2004), and by Côté et al. (2006) and Ferrarese et al. (2006), using HST Advanced Camera for Surveys data for ≈ 100 early-type galaxies in the Virgo cluster (Côté et al. 2004). These analyses show that a majority of these faint galaxies contain a compact stellar cluster at their center. The masses of these star clusters correlate tightly with those of their host galaxies, $M_{\text{CMO}} \approx 0.002 M_{\text{gal}}$, following the same relation between SMBH and galaxy masses seen in more luminous galaxies with $M_{\text{B}} \lesssim -20$ mag (Magorrian et al. 1998; Ferrarese & Merritt 2000; Marconi & Hunt 2003). A correlation between the mass of nuclear star clusters and galaxy properties holds not only in elliptical galaxies, but also in spiral galaxies with bulges (Balcells et al. 2003; Rossa et al. 2006). Nuclear star-clusters with masses in the range $\sim 10^6 - 10^8 M_{\odot}$ have also been found in a handful of bulgeless spiral galaxies (Walcher et al. 2005). These findings strongly suggest that the SMBHs in massive galaxies and the compact stellar nuclei in less luminous galaxies may form as a result of similar physical processes, linked to the formation of the galaxy as a whole.

Many models have been proposed for the observed SMBH-bulge correlations, as reviewed by Robertson et al. (2006a), notably including self-regulation by global feedback, which suppresses further accretion and star formation (e.g., Silk & Rees 1998; Haehnelt et al. 1998; Fabian 1999; King 2003; Wyithe & Loeb 2003; Di Matteo et al. 2005; Springel et al. 2005b; Sazonov et al. 2005; Murray et al. 2005; Wyithe & Loeb 2005); as well as environmental reg-

ulation (e.g., Burkert & Silk 2001; MacMillan & Henriksen 2002; Adams et al. 2001; Balberg & Shapiro 2002; Miralda-Escudé & Kollmeier 2005; Begelman & Nath 2005); and star formation models in which gas dissipation affects the growth of the SMBHs (e.g., Archibald et al. 2002; Di Matteo et al. 2003; Kazantzidis et al. 2005). In particular, self-regulated models with SMBH feedback of photoionization and Compton heating (Sazonov et al. 2005), or in the form of thermal energy coupled to the ambient gas have been demonstrated to successfully reproduce many observed properties of elliptical galaxies formed by major mergers, including the $M_{\text{BH}}-\sigma$ relation (Di Matteo et al. 2005; Robertson et al. 2006b), galaxy colors (Springel, Di Matteo, & Hernquist 2005a), X-ray gas emission (Cox et al. 2006b), quasar properties and luminosity functions (Hopkins et al. 2006a,b), as well as the luminous quasars observed at the highest redshift (Li et al. 2006a).

However, self-regulated models are applicable primarily to galaxies with SMBHs (i.e., massive elliptical galaxies). The new observations by Côté et al. (2006), Ferrarese et al. (2006) and Wehner & Harris (2006) show that many low- and intermediate-mass galaxies that do not appear to have SMBHs still have central compact stellar clusters that obey, to within observational errors, an indistinguishable mass correlation with their host galaxy. This suggests that galactic black holes and central compact stellar nuclei, hereafter collectively referred to as compact massive objects (CMOs), a terminology first introduced by Côté et al. (2006), may have formed from the same processes — gravitational collapse of a massive clump of gas at the center of the galaxy. Furthermore, it suggests that the CMO-host mass correlation may be universal, regardless of galaxy type or mass.

In order to test this hypothesis, we start our investigation of CMOs with bulgeless spirals, which are the simplest galaxy models, and therefore ideal to study the physical process of CMO formation. Nuclear star clusters have been observed in bulgeless spirals by Böker et al. (2002, 2004) and Walcher et al. (2005, 2006). These authors find that the growth of the CMOs is closely linked to the star formation history of the host galaxy. We here examine the CMO-host mass correlation in simulations of isolated, bulgeless disk galaxies with a wide range of masses and gas fractions. We then further investigate how the CMO-host relation changes in simulations of mergers between spiral galaxies.

The rest of this paper is organized as follows. In § 2, we describe our computational methods, galaxy models and parameters. In § 3, we study the formation and evolution of CMOs in isolated, bulgeless, spiral galaxies. We then study the formation of CMOs in mergers between disk galaxies in § 4. We discuss the connections between CMOs and host galaxies in both spirals and ellipticals, and conclude in § 5.

2. COMPUTATIONAL METHOD

We use the publicly available, three-dimensional, parallel, N-body/smoothed particle hydrodynamics (SPH) code GADGET v1.1 (Springel et al. 2001), modified to include absorbing sink particles (Bate, Bonnell, & Price 1995) to directly measure the mass of gravitationally collapsing gas. Li, Mac Low, & Klessen (2005b) and Jappsen et al. (2005) give detailed descriptions of sink particle implementation and interpretation. Sink particles replace gravitationally bound regions of converging flow that reach number densities $n_{\text{sink}} > 10^3 \text{ cm}^{-3}$. The sink particles have a control volume with a fixed radius of 50 pc from which they absorb surrounding

TABLE 1
SPIRAL GALAXY MODELS AND NUMERICAL PARAMETERS

Model ^a	R_{200} ^b	M_{200} ^c	f_g ^d	R_d ^e	h_g ^f	m_g ^g	LT ^h	HT ⁱ
SG50-1	71.43	4.15	0.2	1.41	10	0.21	Y	N
SG50-2	71.43	4.15	0.5	1.41	10	0.21	Y	N
SG50-3	71.43	4.15	0.9	1.41	10	0.37	Y	N
SG50-4	71.43	4.15	0.9	1.07	10	0.75	Y	Y
SG100-1	142.86	33.22	0.2	2.81	10	0.66	Y	N
SG100-2	142.86	33.22	0.5	2.81	10	1.65	Y	N
SG100-3	142.86	33.22	0.9	2.81	10	2.97	Y	Y
SG100-4	142.86	33.22	0.9	2.14	20	5.94	Y	Y
SG120-3	171.43	57.4	0.9	3.38	20	5.17	N	Y
SG120-4	171.43	57.4	0.9	2.57	30	10.3	N	Y
SG160-2	228.57	136.0	0.5	4.51	20	6.80	N	Y
SG160-3	228.57	136.0	0.9	4.51	30	12.2	N	Y
SG160-4	228.57	136.0	0.9	3.42	40	16.3	N	Y
SG220-1	314.29	353.7	0.2	6.20	20	7.07	Y	Y
SG220-2	314.29	353.7	0.5	6.20	30	14.8	N	Y
SG220-3	314.29	353.7	0.9	6.20	40	15.9	N	Y
SG220-4	314.29	353.7	0.9	4.71	40	16.0	N	Y

^a Model of single disk galaxy. First number is rotational velocity in km s^{-1} at the virial radius, the second number indicates sub-model. Sub-models have varying fractions m_d of total halo mass in their disks, and given values of f_g . Sub-models 1–3 have $m_d = 0.05$, while sub-model 4 has $m_d = 0.1$.

^b Virial radius in kpc within which the mean mass density of the halo is 200 times of the critical density.

^c Virial mass of the galaxy in $10^{10} M_{\odot}$.

^d Fraction of disk mass in gas.

^e Radial disk scale length in kpc where stellar surface density drops by e^{-1} .

^f Gravitational softening length of gas in pc.

^g Gas particle mass in units of $10^4 M_{\odot}$.

^h Model run with LT mode $c_s = 6 \text{ km s}^{-1}$.

ⁱ Model run with HT mode $c_s = 15 \text{ km s}^{-1}$.

TABLE 2
GALAXY MERGERS AND NUMERICAL PARAMETERS

Model ^a	$V_{200}(1)$ ^b	$M_{200}(1)$ ^c	$V_{200}(2)$ ^d	$M_{200}(2)$ ^e	f_g ^f	h_g ^g	m_g ^h	c_s ⁱ
MG1	50	4.15	50	4.15	0.2	10	0.37	6
MG2	100	33.22	100	33.22	0.2	10	0.66	6
MG3	100	33.22	100	33.22	0.9	10	2.97	6
MG4	160	136.0	202	272.0	0.1	30	16.0	10
MG5	220	353.7	220	353.7	0.2	40	20.0	6

^a Model of galaxy mergers. Note all progenitors have disk mass fraction of $m_d = 0.05$.

^b Rotational velocity in km s^{-1} at the virial radius for the first progenitor.

^c Virial mass of the first progenitor in $10^{10} M_{\odot}$.

^d Rotational velocity in km s^{-1} at the virial radius for the second progenitor.

^e Virial mass of the second progenitor in $10^{10} M_{\odot}$.

^f Gas fraction of the progenitors.

^g Gravitational softening length of gas in pc.

^h Gas particle mass in units of $10^4 M_{\odot}$.

ⁱ Sound speed for the gas in km s^{-1} .

bound gas. They interact gravitationally and inherit the mass, and linear and angular momentum of the gas they accrete.

2.1. Galaxy Models

Our models of isolated, bulgeless spiral galaxies consist of a dark matter halo following the prescription of (Navarro, Frenk, & White 1997), and an initially exponential disk of stars and isothermal gas. The galaxy structure is based on the analytical work by Mo, Mao, & White (1998), as implemented numerically by Springel & White (1999) and

Springel (2000). The detailed description of the models and numerical simulations are given in Li et al. (2005b). Table 1 lists the most important model properties and numerical parameters. In order to sufficiently resolve gravitational collapse, the models are set up to satisfy three numerical criteria: the Jeans resolution criterion (Bate & Burkert 1997; Whitworth 1998), the gravity-hydro balance criterion for gravitational softening (Bate & Burkert 1997), and the equipartition criterion for particle masses (Steinmetz & White 1997). We choose the particle number for each model such that they not only satisfy the criteria, but also all runs have at least 10^6 total particles. The gas, halo and disk particles are distributed with number ratio $N_g : N_h : N_d = 5 : 3 : 2$. The gravitational softening lengths of the halo $h_h = 0.4$ kpc and disk $h_d = 0.1$ kpc, while that of the gas h_g varies with models. The minimum spatial and mass resolutions in the gas are given by h_g and twice the kernel mass ($\sim 80m_g$). We adopt typical values for the halo concentration parameter $c = 5$, spin parameter $\lambda = 0.05$, and Hubble constant $H_0 = 70 \text{ km s}^{-1} \text{ Mpc}^{-1}$ (Springel 2000).

To test the effects of feedback, we have chosen two values of the isothermal sound speed from the range of velocity dispersions typically observed for neutral gas in disk galaxies $6\text{--}15 \text{ km s}^{-1}$ (Elmegreen & Scalo 2004; Dib et al. 2006). Models designated as low-temperature (LT) have $c_s = 6 \text{ km s}^{-1}$, while high-temperature (HT) models have $c_s = 15 \text{ km s}^{-1}$. We should emphasize that the effective temperature approach we use in our simulations should be regarded as a simple approximation of the underlying processes maintaining the interstellar turbulence level, including stellar feedback, magnetorotational instability, and other processes (see Mac Low & Klessen 2004 for a review). All of the galaxy models have been simulated in the HT mode. However, in our simulations, low mass HT models (e.g., some of the SG50 and SG100 models) do not appear to collapse in the first 3 Gyrs. Only a limited number of runs have been performed in LT mode, as it is prohibitively expensive to run high-mass LT models because they require $\sim 10^7$ particles to fully satisfy the three numerical criteria. The model properties and numerical parameters are summarized in Table 1.

The same set of simulations of isolated galaxies has successfully reproduced many observations of star formation in disk galaxies, including distributions and morphologies (Li et al. 2005b), and both global and local Schmidt laws (Li, Mac Low, & Klessen 2006b), demonstrating that star formation in galaxies are controlled by gravitational instability (Li, Mac Low, & Klessen 2005a). In this paper, we focus on the connection between the CMO and the host galaxy.

In order to investigate CMOs in elliptical galaxies, we have also done five representative models of mergers of spiral galaxies that result in elliptical galaxies. These mergers vary in the mass ratio of the merging pair, progenitor size, gas fraction, effective sound speed, bulge component, and orbital parameters and configuration. Model MG4 resembles the merger of Milky Way and Andromeda, in which the progenitor properties and orbital parameters are set up following Dubinski, Mihos, & Hernquist (1996) and Springel (2000). The mass ratio of the progenitors is roughly 1:2, and each progenitor has a bulge with a mass that is 25% of the disk mass, but neither progenitor initially has a CMO. The two galaxies are on a parabolic orbit, with an initial separation of 700 kpc, and a pericentric distance of 5 kpc. The rest of the models are equal mass, head-on mergers of identical bulgeless progeni-

tors using models SG50-1, SG100-1, SG100-3, and SG220-1, respectively. These mergers are run with parabolic orbits having pericentric distance of 1 kpc, whose separation is the sum of the virial radii of the two progenitors. Each of the mergers is run with particle number around $N_{\text{tot}} \approx 2 \times 10^6$. The model properties and numerical parameters of the merger runs are listed in Table 2. We have also performed a resolution study for the LT versions of models SG100-1 and SG220-1, running each with total particle numbers of 10^5 , 8×10^5 , and 6.4×10^6 , in addition to the standard value of 10^6 . These models cover a factor of four in linear resolution.

2.2. Interpretation of Sink Particles as Clusters and Central Massive Objects

The absorbing sink particles in our models trace regions with pressure of $P/k \sim 10^7 \text{ K cm}^{-3}$, and reach masses of $\gtrsim 10^6 M_\odot$, typical of star-forming proto-stellar clusters (Elmegreen & Efremov 1997). We therefore interpret the formation of sink particles in general as representing the formation of massive stellar clusters. We find in the simulations, however — both in the case of isolated galaxies and for galaxy mergers — that the most massive sink particle always resides in the center of the isolated disk (Li et al. 2005b) or the merger remnant (Li, Mac Low, & Klessen 2004). It either forms there, or migrates to the center quickly after formation due to dynamical friction. We therefore distinguish this sink particle from the others, and identify it as a CMO.

To quantify star formation, we assume that individual sinks represent dense molecular clouds that form stars at some efficiency. Observations by Rownd & Young (1999) suggest that the local star formation efficiency (SFE) in molecular clouds remains roughly constant. Kennicutt (1998) found SFE of 30% for starburst galaxies that Wong & Blitz (2002) showed are dominated by molecular gas. We therefore adopt a fixed local SFE of 30% to convert the mass of sinks to stars, while making the simple approximation that the remaining 70% of the sink particle mass remains in gas form. This conversion rate was shown to reproduce both the global and local Schmidt laws observed in nearby galaxies (Li et al. 2006b).

We assume, on the other hand, that the CMO inherits the total mass of the central sink particle, for the following reasons. (1) If the CMO forms a compact stellar cluster, then the star formation efficiency could be $> 50\%$ due to extremely high pressure and density at the galactic center (Elmegreen & Efremov 1997), where the deep gravitational potential also helps to keep the gas bound the CMO. (2) If a fraction of the CMO collapses into a black hole, then it could rapidly accrete the remaining gas. (3) Although feedback-driven winds from either supernovae or a quasar could expel the gas from galactic nuclei, the effect may be minor. A study of galactic winds by Cox et al. (2006a) shows that the mass loss by a typical stellar wind (wind efficiency ~ 0.5 , wind velocity $\sim 500 \text{ km s}^{-1}$) is less than 10% of the initial total gas mass. The quasar outflow is comparable to this in galaxies with accreting black holes. Furthermore, most of the gas in the central region is consumed quickly by either star formation or black hole accretion, so the mass loss from the CMO by feedback is likely negligible (Cox et al. 2006b).

The final mass and fate of the CMO should depend on the galaxy potential and dynamical evolution. The larger the galaxy, the more massive its central clump, due to stronger gravitational instability (Li et al. 2005a). The gas clump may then form a supermassive black hole directly by rapid core

collapse within a deep potential well, fragment to form a massive star cluster in a less-massive galaxy, or engage in cluster-cluster collisions to form a SMBH in galaxy mergers due to stellar dynamical processes (see, e.g., Rees 1984 and Haiman & Quataert 2004 for reviews of different routes to forming a SMBH). Furthermore, the $M_{\text{CMO}}-M_{\text{gal}}$ relation may be established by the same physical mechanism that determines the fate of the clump — massive galaxies or galaxy mergers that have higher CMO mass tend to form stars at a higher rate than less massive ones. These considerations suggest that the $M_{\text{CMO}}-M_{\text{gal}}$ relation is directly connected to the star formation efficiency of the galaxy.

In the simulations, we do not resolve the transition within the sink particle from a collapsed gas clump to a black hole or a star cluster, and consequently we will limit our discussion, and comparisons to observations, to CMOs in general.

3. CENTRAL MASSIVE OBJECTS IN BULGELESS SPIRAL GALAXIES

3.1. The Formation and Evolution of CMOs

In all of our simulations, high gas density regions collapse to form stars and clusters once the disk becomes gravitationally unstable. Sink particles first form in the central regions of galaxies; star formation subsequently propagates outwards. The collapsed objects continue to grow by gas accretion.

The growth histories of CMOs in several models were shown in Figure 1. The CMO initially collapses at a mass above the Jeans mass ($M_J \sim 10^6 M_\odot$ and $\sim 2 \times 10^7 M_\odot$ for LT and HT models, respectively). We find that in the first few hundred million years, the CMO grows rapidly, accreting gas particles gravitationally bound to it, at a rate that is within an order of magnitude of the spherical Bondi-Hoyle accretion rate (Hoyle & Lyttleton 1941; Bondi & Hoyle 1944; Bondi 1952):

$$\dot{M}_{\text{BH}} = \frac{4\pi\alpha G^2 M_{\text{CMO}}^2 \rho}{(c_s^2 + v^2)^{3/2}} \quad (1)$$

where M_{CMO} is the CMO mass, ρ and c_s are the density and sound speed of the gas, respectively, α is a dimensionless parameter of order unity, and v is the velocity of the CMO relative to the gas. After the initial accretion period, the growth slows down. In about 1 Gyr, the masses of most CMOs saturate due to the depletion of gas around the nucleus by star formation, as shown in the middle panel of Figure 1. We note that a study by Sazonov et al. (2005) of radiative feedback from accreting black holes in ellipticals shows that the observed $M_{\text{BH}}-\sigma$ relationship could be established once most ($> 99\%$) of the gas has been converted into stars. This finding agrees with our results that the growth of the CMO is tied to the star formation in the galaxy.

The resolution studies show that the masses of the CMOs converge to better than a factor of two in runs with particle numbers $\geq 10^6$ for both models SG100-1 and SG220-1, in which just the gas particle mass is smaller than the Jeans mass at which the CMO collapses initially. We include in our analysis two models that satisfy this requirement in order to extend the range of LT models that we can consider, as we will discuss.

3.2. The $M_{\text{CMO}}-M_{\text{gal}}$ Correlation

In Figure 2, we show the correlation between the mass of CMO and that of the host for the bulgeless, isolated disk models. We consider three different definitions of galaxy

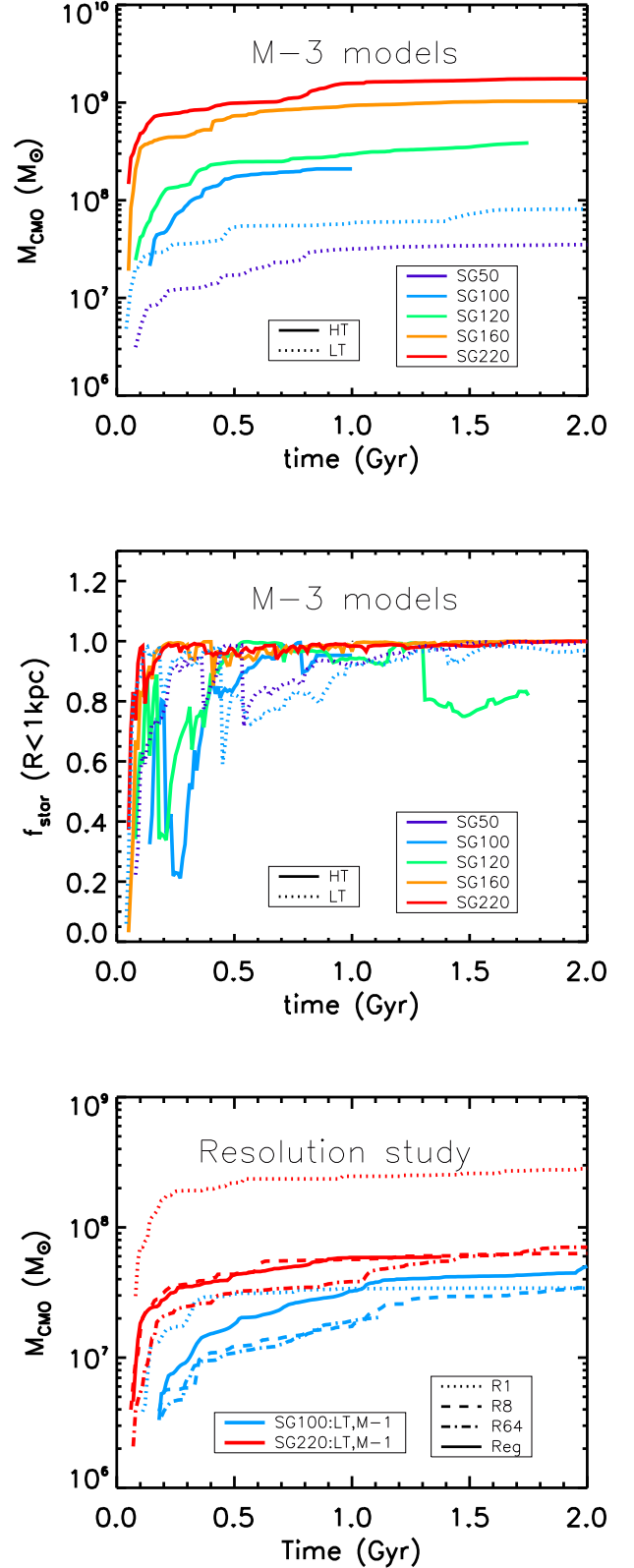


FIG. 1.— Mass growth histories of the CMOs in selected galaxy models (top panel), and the stellar mass fraction in the nuclear region within 1 kpc of the galactic center (middle panel). Also shown are the histories of CMO mass from the resolution study (bottom panel). The designations R1, R8, R64 and Reg indicate total particle numbers of 10^5 , 8×10^5 , 6.4×10^6 , and 10^6 , respectively.

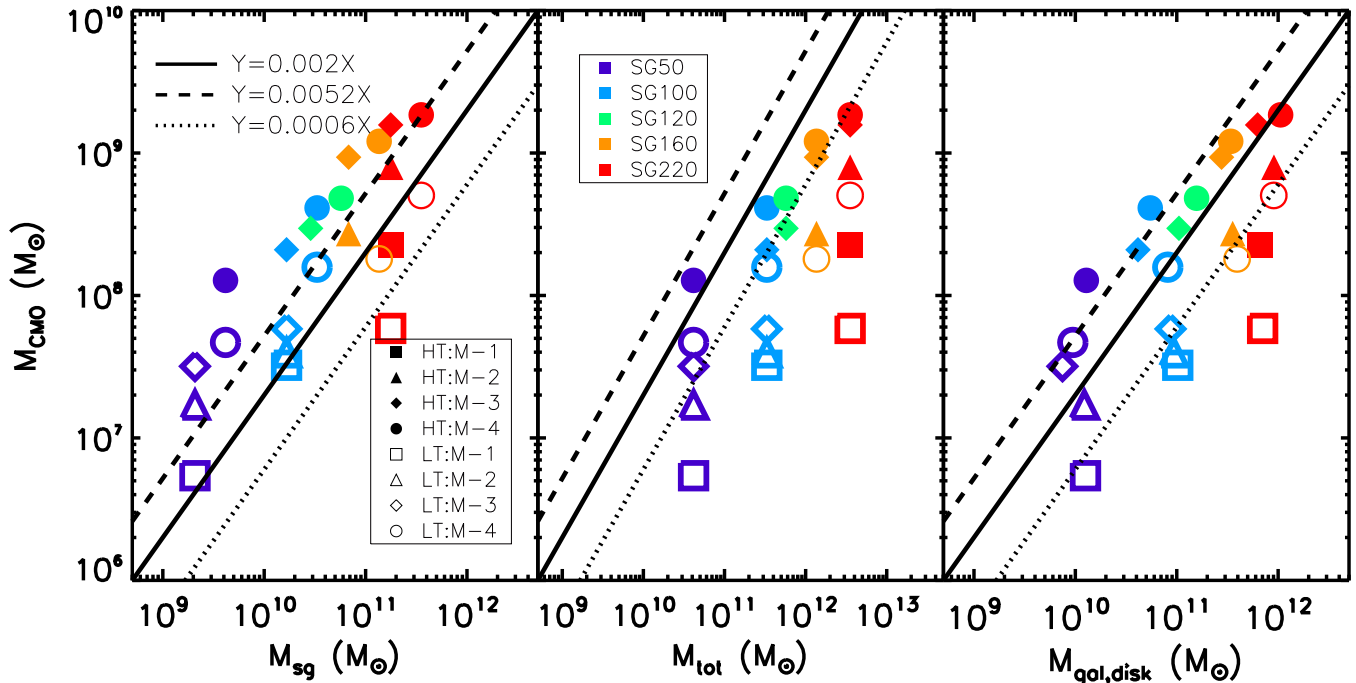


FIG. 2.— The relation between CMO mass and host mass in simulated bulgeless spiral galaxies. Galaxies are shown from both the LT (*open symbols*) and HT (*filled symbols*) models. The color and the shape of the symbol indicates the rotational velocity and sub-model (gas fraction and disk scale length) for each galaxy described in Table 1. The solid line is the best fit to spheroid systems observed by Ferrarese et al. (2006), while the dotted line and the dashed line indicate the observed range. We show three different characterizations of the host mass, as discussed in the text: (*left*) M_{sg} the mass of both stars and gas; (*middle*) M_{tot} the total mass; and (*right*) $M_{\text{gal,disk}}$ the total mass within the half-mass radius. The last definition produces a scaling relation close to that observed between SMBHs and stellar spheroids (Ferrarese et al. 2006), suggesting that it may be the closest analog of the mass M_{gal} used by Cappellari et al. (2006) to characterize bulgeless spirals. Note that the two LT models in *thin* circles, SG160-4 and SD220-4 do not fully satisfy the Jeans criterion, but judging from our resolution study, likely represent upper limits to the CMO mass. See § 3.2 for details.

mass: M_{sg} , the combined mass of stars and gas, M_{tot} , the total mass of the galaxy including stars, gas, and dark matter, and $M_{\text{gal,disk}}$, the total mass of the galaxy within $5R_e$, where R_e is the half-light radius, containing half of the gas and stellar mass of the disk component. In all three cases, M_{CMO} is measured after 1 Gyr, or in the few cases where the simulations stopped before 1 Gyr, at the last time step. The two LT models SG160-4 and SD220-4 (shown in thin circles) do not fully satisfy the Jeans criterion (i.e., the SPH kernel mass of 32 gas particles is smaller than the Jeans mass) due to computation limit. However, from the resolution study in Figure 1, the CMO mass converges to roughly a factor of two even in runs where the gas particle mass is smaller than the initial CMO mass. We believe that these models represent the upper limits of the CMO mass of these two models.

Figure 2 shows that for any definition of the galaxy mass, the mass of CMO correlates strongly with the mass of its host, despite the lack in our models of any explicit feedback from the CMO. It also appears that the correlation has a similar normalization and linear slope to that found for both star clusters and SMBHs.

In reality, the neutral gas velocity dispersion in individual galaxies typically has a range of $6-15 \text{ km s}^{-1}$ so the scatter in the $M_{\text{CMO}}-M_{\text{gal}}$ relation, represented by the combination of the LT and HT runs, may reflect the range of effective temperature we use here. Because the masses of the CMOs depend on the effective sound speed of the gas, it is desir-

able to have a wide range of models with different effective sound speeds. Nevertheless, from the models we have simulated, there is reasonable overlap of the two (LT and HT) temperature regimes, as shown in Figure 2. This suggests that the $M_{\text{CMO}}-M_{\text{gal}}$ relation is similar for different temperatures, apart from a factor of ≈ 2 shift in the overall normalization, independent of host mass.

It would be interesting to compare these findings directly with the observations, but such a comparison is difficult at present. Walcher et al. (2005) have determined the masses of nuclear star clusters in 9 bulgeless spiral galaxies, and found them to range between $8 \times 10^5 M_{\odot}$ and $6 \times 10^7 M_{\odot}$. These appear a factor of several smaller than the masses of the CMOs we find in galaxies with $M_{\text{tot}} = 10^{11} - 10^{12} M_{\odot}$, but the masses of the hosts in their sample are not discussed, and their sample may also suffer from selection biases.

Other comparisons are possible, but have to be interpreted with caution, since it is not clear how to relate the bulgeless disks in these models to the spheroid components that are found to correlate with CMOs in other observations. Nevertheless, we present here two such brief comparisons:

(1) Balcells et al. (2003) and Rossa et al. (2006) study late-type spirals with bulges. They find that the masses of the CMO at fixed bulge luminosity is about 3 times above the mass expected from the M_{BH} vs. L_{bulge} relation (Marconi & Hunt 2003). In the left panel of Figure 2, we find a similar offset (relative to the $M_{\text{BH}}-M_{\text{bulge}}$ relation), if

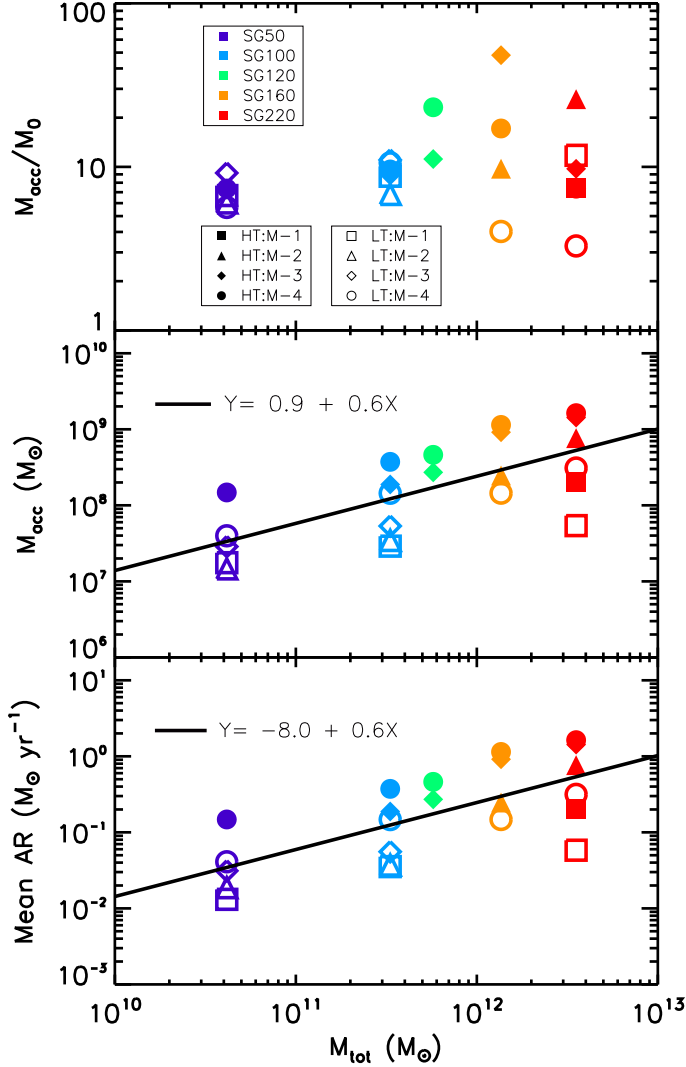


FIG. 3.— This figure shows how the CMOs gain mass, as a function of total galaxy mass M_{tot} . The *top panel* shows the ratio of the accreted mass M_{acc} to the initial collapsed seed mass M_0 , while *middle* and *bottom* panels show M_{acc} and mean accretion rate of the CMO, respectively, as functions of M_{tot} of the galaxy. The mean accretion rate is the average over 1 Gyr (or the maximum simulation time if shorter) when M_{CMO} is measured, as explained in the text. The symbols are the same as in the previous plots, while the solid line is the least-square fit to the data.

the total baryon mass is considered as a proxy for the bulge mass. One possible rationale for this comparison is that most of the baryon content of our simulated bulgeless disk galaxy may represent the stars making up the bulge of any galaxy that subsequently forms out of this bulgeless spiral.

(2) Côté et al. (2006); Ferrarese et al. (2006) and Wehner & Harris (2006) study early-type galaxies, and find a correlation between the masses of the CMOs and the host galaxies. In particular, Ferrarese et al. define M_{gal} , following the formula given by Cappellari et al. (2006), as $M_{\text{gal}} = \alpha R_e \sigma^2 / G$, where G is the gravitational constant, σ is the observed velocity dispersion, and $\alpha = 5$ is a constant. This typically represents ~ 0.25 of the total galaxy mass (see

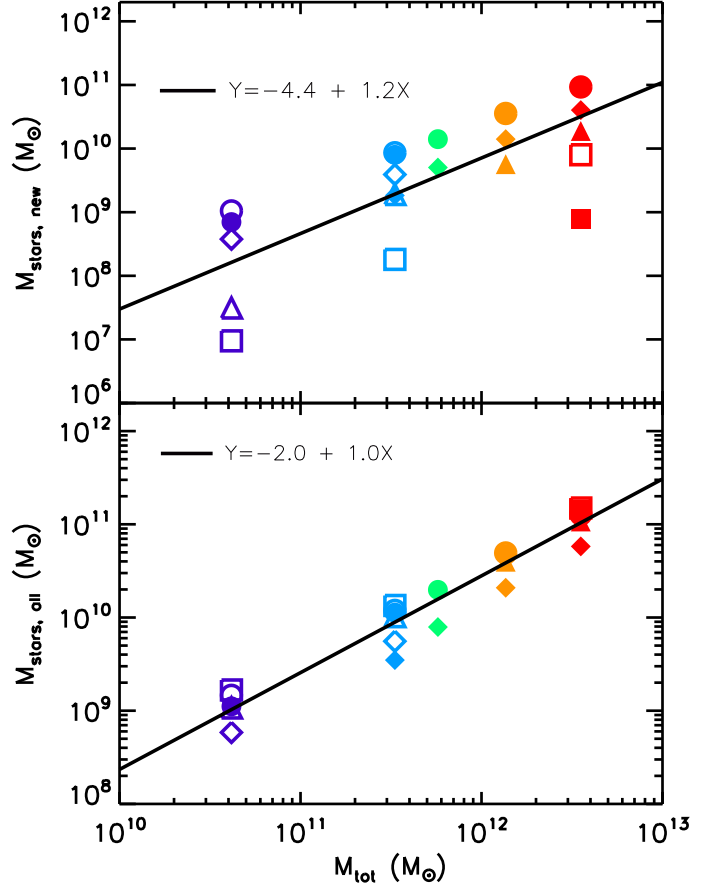


FIG. 4.— Stellar mass of the galaxy as a function of total galaxy mass M_{tot} . The *top panel* shows the mass of newly formed stars (30% of the sink particles formed in the simulation, aside from the CMO), while the *bottom panel* shows the mass of all stars, including both newly formed ones and the old disk stars.

below). Our definition of $M_{\text{gal,disk}}$ is designed to mimic this quantity, and, as the right panel of Figure 2 shows, we find, within errors, that our bulgeless disk galaxies obey the same correlation.

Both of the above comparisons suggest that the $M_{\text{CMO}}-M_{\text{gal}}$ relation established in our simulated bulgeless disk galaxies may evolve into the observed correlation between M_{CMO} and their spheroid host, once the bulgeless disk galaxy (or a fraction of its mass) evolves into a spheroid. Establishing a direct connection, however, is not possible without modeling in detail the further evolution of both the host galaxy and the CMO (the latter, of course, may also gain mass). We next turn to CMOs that form in our simulations of merging galaxies.

3.3. Toward a Physical Explanation of the $M_{\text{CMO}}-M_{\text{gal}}$ Correlation

The physics responsible for the mass correlation, in general, must be tied to the formation of a seed CMO, and its subsequent growth by accretion. To investigate this issue further, we define the initial collapsed seed CMO mass as M_0 , and the accreted mass as M_{acc} . The final CMO mass is the sum of these two, $M_{\text{CMO}} = M_0 + M_{\text{acc}}$, where M_0 is essentially the local Jeans mass. Our sink particles form at a fixed, arbitrary

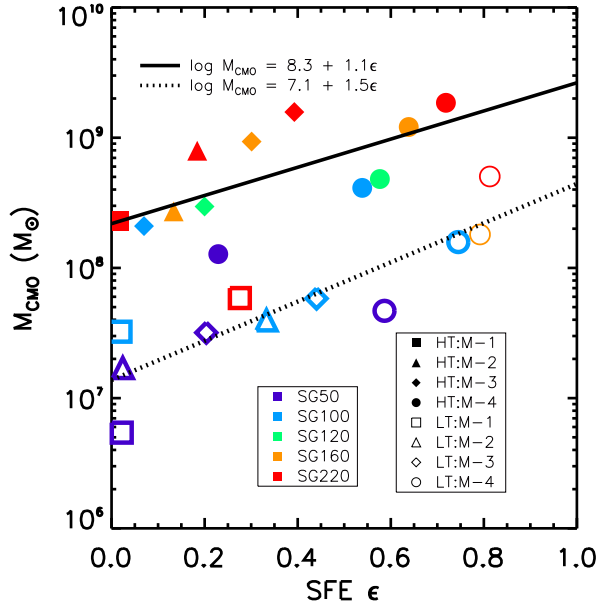


FIG. 5.— Correlation between the mass of the CMO and the global star formation efficiency in the galaxy in different models. Symbols are the same as in Figure 2. The black lines show a least-square fit to the data points from models of each temperature. Because the CMO mass depends on the effective sound speed, so the lower Jeans masses in the LT runs result in a higher global SFE, and a smaller CMO. Our choice of two discrete values of c_s represents the range of scattering (see text for more discussions).

density n_{sink} , and our models have a sound speed chosen from one of two values, so unsurprisingly, CMOs in galaxies with the same sound speed have a similar value of M_0 . However, we find that $M_{\text{acc}} \gg M_0$; that is, subsequent accretion plays a much more important role in determining the final mass of the CMO than initial collapse, as shown in Figure 3 (*top panel*).

Figure 3 shows that M_{acc} and the average accretion rate of the CMO increase on average with the total mass of the galaxy M_{tot} (*middle and bottom panels*). We expect the CMOs to accrete at roughly the Bondi (1952) rate (eq. 1), so a more massive or gas-rich galaxy that has higher gas density, which enables higher accretion rate, ought to have higher values of M_{CMO} .

Indeed, at fixed CMO mass and sound speed, equation (1) shows $\dot{M}_{\text{BH}} \propto \rho$. In a rotating disk in hydrostatic equilibrium, the characteristic density scales as $\rho \propto M_{\text{tot}}^{2/3}$ (Wood & Loeb 2000), assuming that the disk mass and scale radius are fixed fractions of the total galaxy mass M_{tot} and size $R \propto M_{\text{tot}}^{1/3}$. Hence, we expect $\dot{M}_{\text{BH}} \propto M_{\text{tot}}^{2/3}$, close to the power-law index of 0.6 seen in the bottom panel in Figure 3. On the other hand, the gas-depletion time-scale τ_d , which halts both star-formation and the growth of the CMO, depends weakly on M_{gal} (see Fig. 1). This leads us to a qualitative understanding of the $M_{\text{CMO}}-M_{\text{gal}}$ correlation seen in Figure 2. Since the CMO mass is dominated by accretion, we can very roughly approximate it as $M_{\text{CMO}} \simeq \dot{M}_{\text{BH}}\tau_d \propto M_{\text{tot}}^{2/3}$, while $M_{\text{gal,disk}}$ is roughly dependent on the stellar mass of the galaxy. As shown in Figure 4, M_{star} increases linearly with M_{tot} , $M_{\text{star}} \propto M_{\text{tot}}$. This generally supports the observed positive correlation of $M_{\text{CMO}}-M_{\text{gal}}$. Although this argument does not fully explain the observed linear relationship, it does ignore several factors

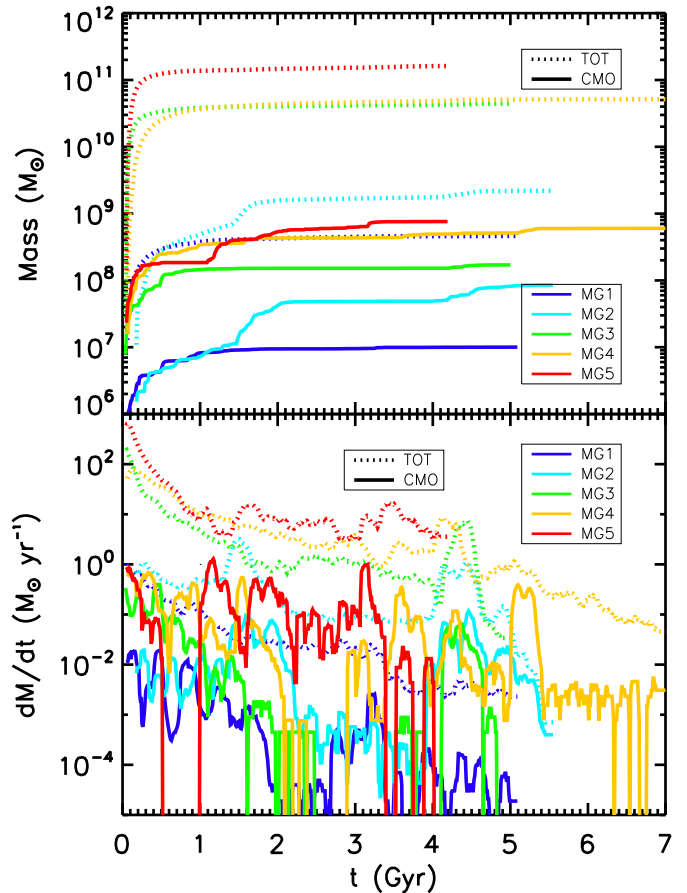


FIG. 6.— History of CMO (*solid*) and total collapsed (*dotted*) mass (*top*) and accretion rate (*bottom*) in all five galaxy mergers. Total mass collapsed counts mass in all sink particles, a quantity related to the total amount of star formation in the galaxy by the local star formation efficiency.

that likely depend at least weakly on M_{tot} , including the dark matter contribution to the galactic disk.

The final mass of the CMO correlates tightly with the *global* star formation efficiency of the galaxy, with a normalization dependent on the effective sound speed, as shown in Figure 5. This further demonstrates a close link between the growth of the CMO and the build-up of the host galaxy through star formation. The dependence of the CMO mass on the effective sound speed can be understood from Bondi-Hoyle accretion. The initial mass of the CMO is close to the Jeans mass of the collapsing gas, $M_{\text{CMO}} \propto M_J \propto \rho^{-1/2}c_s^3$, so $\dot{M}_{\text{BH}} \propto c_s^3$. Because of this strong dependence on the sound speed, our choice of two discrete values of c_s at extremes of the expected range produces the discrete behavior seen in Figure 5. In reality, we would expect a scatter between these extremes.

4. CENTRAL MASSIVE OBJECTS IN GALAXY MERGERS

Previous simulations have demonstrated that major mergers of spiral galaxies generally trigger starbursts and produce elliptical galaxies (e.g., Toomre & Toomre 1972; Hernquist 1989; Barnes & Hernquist 1992; Hernquist 1992; Mihos & Hernquist 1996; Dubinski, Mihos, & Hernquist 1999; Springel 2000; Barnes 2002; Naab & Burkert 2003;

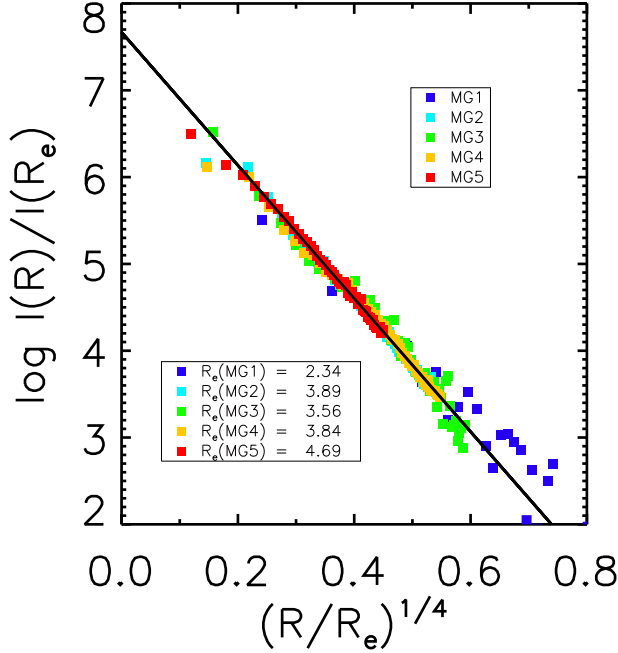


FIG. 7.— Surface brightness profiles of all five merger remnants at the end of the simulations indicated in Figure 6. All five models fit well to a (Sérsic 1963, 1968) profile with $m = 4$ (black line), as explained in the text. The legend gives the effective radius R_e of each model.

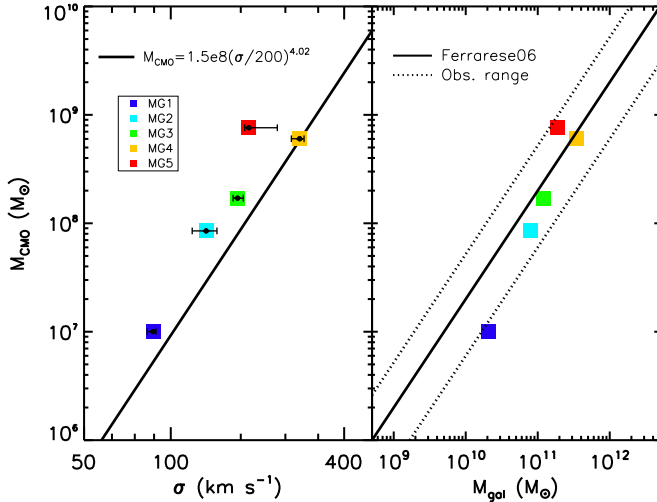


FIG. 8.— The relations between CMO mass and host mass and velocity dispersion at the conclusion of our galaxy merger models. The value of M_{CMO} is the final mass of the CMO after completion of mergers, the σ is taken at the mean values, and the error bar indicates the range over 10^4 viewing angles. The calculation of M_{gal} is described in the text. The black curve in the left panel indicates the best fit to observations by Tremaine et al. (2002), while those in the right panel are from observations by Ferrarese et al. (2006).

Li et al. 2004). Recently, simulations of galaxy mergers that include SMBHs have been carried out to investigate the SMBH-spheroid relations. Although some dissipationless simulations showed that the $M_{\text{BH}}-\sigma$ relation could be maintained for mergers with modest energy and angular momentum (Nipoti et al. 2003; Boylan-Kolchin et al. 2005), it was pointed out that gas dissipation and star formation are essential to this correlation (Kazantzidis et al. 2005). In particular, Di Matteo et al. (2005) suggest that thermal feedback from an SMBH suppresses both black hole accretion and star formation, giving the $M_{\text{BH}}-\sigma$ correlation in ellipticals. Together, these studies suggest that the SMBH-spheroid correlations are closely connected to star formation, and that it may play a dominant role in determining the masses of SMBH and spheroids.

In previous simulations, SMBHs are initialized in the progenitors following the $M_{\text{BH}}-\sigma$ correlation. In our merger simulations, CMOs form dynamically as the galaxies evolve, in the same manner as in our models of isolated spirals. The growth histories of the CMOs in our merger models are shown in Figure 6. Because only the most massive CMO is considered in the merger remnants, the CMO in galaxy mergers is identified as the most massive one. Similar to the isolated disk galaxies, the mass curves of the CMO increase rapidly in the initial phase. However, the detailed accretion history is modulated by the interaction between the progenitors. Close encounters trigger episodes of very high accretion rate, both on local and global scale, as shown in the bottom panel of Figure 6. The mass curves saturate after the completion of the mergers.

In order to investigate the $M_{\text{CMO}}-\sigma$ correlation between the CMOs and the merger remnant velocity dispersions, we made simulated observations, following Gebhardt et al. (2000). We measured the surface brightness-weighted, line-of-sight stellar velocity dispersion σ of the spheroid within an aperture of size $R_e/8$, where R_e is the effective radius. As mentioned in Boylan-Kolchin, Ma, & Quataert (2005) and Robertson et al. (2006a), a standard technique for obtaining R_e is to fit the projected surface brightness profile, $I(R) = L(R)/(4\pi R^2)$, to a (Sérsic 1963, 1968) profile and derive the half-light radius:

$$I(R) = I(R_e) \exp\{-b(m)[(R/R_e)^{1/m} - 1]\}. \quad (2)$$

where $b(m) \approx 2m - 1/3 + 4/(405m)$, as given by Ciotti & Bertin (1999).

Bulges and early-type galaxies have surface brightness profiles $I(R)$ that are usually well-approximated by the de Vaucouleurs law (de Vaucouleurs 1948)

$$\log I(R)/I(R_e) \propto -(R/R_e)^{1/m} \quad (3)$$

with Sérsic index $m = 4$. Figure 7 shows the surface brightness profiles $I(R)$ of all three of our merger remnants, assuming a fixed mass-to-light ratio of three. These profiles appear to follow the $m = 4$ de Vaucouleurs law (de Vaucouleurs 1948) closely, as also found by Hernquist (1992) who studied mergers of bulgeless spiral progenitors. We note that Balcells et al. (2003) and Graham et al. (2005) proposed a smaller index, $m \sim 1.7-3.5$ for bulges, and it was suggested that only ellipticals with $M_B \leq -21$ mag have $m \simeq 4$ profiles (e.g., Graham & Guzmán 2003). However, the derived value of m from fitting observations appears to depend on the data set and the observed wavelengths. As noted in Balcells et al. (2003), data from HST seems to give a much smaller m (e.g., $m \sim 1.7$) than that from *Spitzer* (e.g., $m \sim 4-6$) for the same

sample, and low Sérsic indices are not expected from galaxy mergers. Graham (2006) reported a correlation between the masses of CMOs and the Sérsic index of the host spheroids in the sample compiled by Ferrarese et al. (2006). More merger simulations with different initial conditions, mass ratios and orbital parameters are necessary to explore this relation.

The effective radius R_e is then derived from the half-light radius of each spheroid, as given in the legend of Figure 7. The mass-weighted line-of-sight stellar velocity dispersion σ within $R_e/8$ is then calculated for each remnant galaxy for 10^4 random viewing angles. Figure 8 shows the resulting correlation of $M_{\text{CMO}}-\sigma$ for the merger remnants. It appears to agree very well with the observational correlation, $M_{\text{BH}} = 1.5 \times 10^8 (\sigma/200 \text{ km s}^{-1})^{4.02} M_\odot$ (Ferrarese & Merritt 2000; Tremaine et al. 2002).

Figure 8 also shows the correlation $M_{\text{CMO}}-M_{\text{gal}}$ between the mass of CMO and M_{gal} of the host for the galaxy mergers. Here M_{gal} is calculated using the virial mass, following Cappellari et al. (2006), $M_{\text{gal}} = \alpha R_e \sigma^2 / G$, where G is the gravitational constant and $\alpha = 5$. This is the best-fitting virial relation based on the observables R_e and σ . The simulation agrees very well with the observed correlation $M_{\text{CMO}} \approx 0.002 M_{\text{gal}}$ (Ferrarese et al. 2006), within the 1σ observational uncertainty, as indicated by the dotted lines in this figure.

5. DISCUSSION AND SUMMARY

Our simulations of gravitational collapse of gas in galaxies enable us to model star formation in galaxies and follow the growth and evolution of CMOs. Our approach differs from previous studies such as Kazantzidis et al. (2005) and Di Matteo et al. (2005) in the following ways.

1. Our resolution is sufficient to fully resolve gravitational collapse.
2. Absorbing sink particles are used to directly follow and measure the mass of gravitationally collapsing gas.
3. In our model, the black holes, or CMOs, are not set up *a priori* according to the $M_{\text{BH}}-\sigma$ correlation as in previous approaches. Instead they form dynamically from gravitational collapse of gas, the same as star clusters, with both being represented by sink particles. In these simulations, the CMO is just the most massive sink particle, which always is found in the galaxy center at the end of our simulations.
4. Our model does not explicitly include feedback from either star formation or black hole formation. However, feedback from star formation is implicitly represented by our isothermal equation of state with relatively high effective sound speed of 6–15 km s⁻¹.

We emphasize that our models do not include explicit feedback, magnetic fields, or gas recycling. However, we believe each will have minor effects on the final mass of the CMO. The assumption of an isothermal equation of state for the gas implies substantial feedback to maintain the effective temperature of the gas against radiative cooling and turbulent dissipation. Real interstellar gas has a wide range of temperatures but the root-mean-square (rms) velocity dispersion generally falls within the range 6–15 km s⁻¹ (e.g., Elmegreen & Scalo 2004; Dib et al. 2006).

At least three effects may conspire to maintain the velocity dispersion in the observed narrow range, as reviewed in

Li et al. (2005b). First, radiative cooling drops precipitously in gas with sound speed $\lesssim 10$ km s⁻¹ as it becomes increasingly difficult to excite the Lyman α line of hydrogen. Second, direct feedback from the starburst may play only a minor role in quenching subsequent star formation (e.g. Kravtsov 2003; Monaco 2004), perhaps because most energy is deposited not in the disk but above it as superbubbles blow out (e.g. Fujita et al. 2003; de Avillez & Breitschwerdt 2004). The energy input \dot{E} from supernovae at the observed Galactic rate drives a flow with rms velocity dispersion of ~ 9.5 km s⁻¹ (de Avillez 2000), and the rms velocity dispersion depends only on $\dot{E}^{1/3}$ (Mac Low 1999; Mac Low & Klessen 2004), so a wide range of star formation rates leads to a narrow range of velocity dispersions. Third, magnetorotational instabilities may maintain a modest velocity dispersion even in the absence of any other feedback (Sellwood & Balbus 1999; Dziourkevitch, Elstner, & Rüdiger 2004).

Radiative feedback from the central SMBH in massive galaxies will only Compton heat the gas much above 10^4 K if the gas is sufficiently ionized. Sazonov et al. (2005) shows that this will occur if the ionization parameter

$$\xi = \frac{L}{nr^2} = 1.4 \times 10^8 \frac{M_{\text{BH}}}{10^8 M_\odot} \frac{1 \text{ cm}^{-3}}{n} \left(\frac{1 \text{ pc}}{r} \right)^2, \quad (4)$$

exceeds $\xi_{\text{crit}} \approx 10^3$, with the Compton temperature of $\sim 10^7$ K being reached only for $\xi \approx 10^5$. In this equation, M_{BH} is the SMBH mass, L is the bolometric luminosity, which is assumed to be a constant fraction one-tenth of the Eddington luminosity, n the number density, and r the distance from the SMBH. If we examine the conditions at the Bondi-Hoyle accretion radius for the SMBH,

$$R_{\text{BH}} = \frac{GM_{\text{BH}}}{c_s^2} \approx (4.5 \text{ kpc}) \frac{M_{\text{BH}}}{10^8 M_\odot} \left(\frac{c_s}{10 \text{ km s}^{-1}} \right)^{-2} \quad (5)$$

we find that gas with a density of $n > (9 \times 10^{-3} \text{ cm}^{-3})(M_{\text{BH}}/10^8 M_\odot)$ will remain at 10^4 K (see also Sazonov et al. 2005). This may contribute to maintaining the sound speed at roughly 10 km s⁻¹ in dense gas further in that might otherwise cool. On the other hand, the heating in the immediate neighborhood of the SMBH may still lead to unsteady accretion as modeled by Ciotti & Ostriker (2001).

We should also emphasize that gas recycling from dying stars is not included in our simulations. As computed explicitly, for example, in Haiman et al. (2004), stars can return over 40% of their mass in gas. However, since the recycled gas might be heated up or blown out by the feedback, it may not be accreted by the CMOs. Our models with different effective sound speeds satisfy similar correlations between M_{CMO} and host galaxy mass (though not the same relation between CMO mass and star formation efficiency). Furthermore, as discussed in § 2.2, the mass loss due to galactic winds is only a small fraction of the initial gas mass, suggesting that the effect of feedback on the mass of the CMO may be minor.

The simple model of sink particles that grow with approximately spherical Bondi-Hoyle accretion reproduces the observed $M_{\text{CMO}}-\sigma$ and $M_{\text{CMO}}-M_{\text{gal}}$ correlations reasonably. Both the accreted mass of CMO and the mass turned into stars scale with the total mass of a galaxy, offering a plausible explanation for the CMO-host relation. We should note that Escala (2006) also reproduces the $M_{\text{BH}}-\sigma$ correlation by

modeling accretion of BHs from a Shakura-Sunyaev thin disk (Shakura & Sunyaev 1973). This suggests that the accretion rates through these two different mechanisms may be similar, and that the final mass of the black hole or the CMO may be largely determined by the depletion of accretable gas. The fact that various previous approaches, including feedback models (e.g. Di Matteo et al. 2005; Sazonov et al. 2005), star formation models (e.g., Kazantzidis et al. 2005), and accretion models (e.g., Escala 2006), have more or less succeeded in reproducing the SMBH-host correlation suggests that gas depletion in the central region is crucial to this correlation. Our results support the idea that star formation plays the major role in gas consumption and determination of the final masses of the CMO and the stellar component.

The close correlation that we find between the CMO mass and global star formation efficiency in the host galaxy suggests that the CMO-host link may be universal, in that it is the result of the co-eval growth and evolution of the CMO and the host galaxy, and therefore it does not strongly depend on the morphology, type, or mass of the galaxy. A systematic search for CMOs in the nuclei of bulgeless disk galaxies would offer a test of this conclusion.

In summary, our simple model of accretion and star formation reproduces quantitatively the observed $M_{\text{BH}}-\sigma$ correlation for galaxy mergers, and suggests a universal $M_{\text{CMO}}-M_{\text{gal}}$ relation over a wide range of galaxy mass and morphological

types. We find that the CMO builds up its mass through accretion, and that there is a direct correlation between the global star formation efficiency of a galaxy and its CMO mass. Our results suggest that star formation may play an important role in producing the fundamental mass correlation between the central massive objects and their host galaxies.

We thank V. Springel for making both GADGET and his galaxy initial condition generator available, as well as K. Gebhardt, A. Graham, L. Hernquist, A. Loeb, J. Ostriker, and E. Quataert for useful discussions and comments on the manuscript. YL thanks L. Hernquist for his encouragement, and is supported by an Institute for Theory and Computation Fellowship. ZH acknowledges partial support by NASA through grants NNG04GI88G and NNG05GF14G, by the NSF through grants AST-0307291 and AST-0307200, and by the Hungarian Ministry of Education through a György Békésy Fellowship. M-MML acknowledges partial support by NASA under grant NAG5-13028, and by the NSF under grants AST-9985392 and AST-0307854. Computations were performed at the Pittsburgh Supercomputer Center supported by the NSF, on the Parallel Computing Facility of the AMNH, and on an Ultrasparc III cluster generously donated by Sun Microsystems.

REFERENCES

- Adams, F. C., Graff, D. S., & Richstone, D. O. 2001, *ApJ*, 551, L31
 Archibald, E. N., Dunlop, J. S., Jimenez, R., Friaça, A. C. S., McLure, R. J., & Hughes, D. H. 2002, *MNRAS*, 336, 353
 Balberg, S., & Shapiro, S. L. 2002, *Physical Review Letters*, 88, 101301
 Balcells, M., Graham, A. W., Domínguez-Palmero, L., & Peletier, R. F. 2003, *ApJ*, 582, L79
 Barnes, J. E. 2002, *MNRAS*, 333, 481
 Barnes, J. E., & Hernquist, L. 1992, *ARA&A*, 30, 705
 Bate, M. R., Bonnell, I. A., & Price, N. M. 1995, *MNRAS*, 277, 362
 Bate, M. R., & Burkert, A. 1997, *MNRAS*, 288, 1060
 Begelman, M. C., & Nath, B. B. 2005, *MNRAS*, 361, 1387
 Böker, T., Laine, S., van der Marel, R. P., Sarzi, M., Rix, H.-W., Ho, L. C., & Shields, J. C. 2002, *AJ*, 123, 1389
 Böker, T., Sarzi, M., McLaughlin, D. E., van der Marel, R. P., Rix, H.-W., Ho, L. C., & Shields, J. C. 2004, *AJ*, 127, 105
 Bondi, H. 1952, *MNRAS*, 112, 195
 Bondi, H., & Hoyle, F. 1944, *MNRAS*, 104, 273
 Boylan-Kolchin, M., Ma, C.-P., & Quataert, E. 2005, *MNRAS*, 362, 184
 Burkert, A., & Silk, J. 2001, *ApJ*, 554, L151
 Cappellari, M., Bacon, R., Bureau, M., Damen, M. C., Davies, R. L., de Zeeuw, P. T., Emsellem, E., Falcón-Barroso, J., Krajnović, D., Kuntschner, H., McDermid, R. M., Peletier, R. F., Sarzi, M., van den Bosch, R. C. E., & van de Ven, G. 2006, *MNRAS*, 366, 1126
 Ciotti, L., & Bertin, G. 1999, *A&A*, 352, 447
 Ciotti, L., & Ostriker, J. P. 2001, *ApJ*, 551, 131
 Côté, P., Blakeslee, J. P., Ferrarese, L., Jordán, A., Mei, S., Merritt, D., Milosavljević, M., Peng, E. W., Tonry, J. L., & West, M. J. 2004, *ApJS*, 153, 223
 Côté, P., Piatek, S., Ferrarese, L., Jordán, A., Merritt, D., Peng, E. W., Haşegan, M., Blakeslee, J. P., Mei, S., West, M. J., Milosavljević, M., & Tonry, J. L. 2006, *ApJS*, 165, 57
 Cox, T. J., Besla, G., Chakrabarti, S., Di Matteo, T., Hernquist, L., Hopkins, P. F., Krause, E., Li, Y., Robertson, B., & Springel, V. 2006a, in preparation
 Cox, T. J., Di Matteo, T., Hernquist, L., Hopkins, P. F., Robertson, B., & Springel, V. 2006b, *ApJ*, 643, 692
 de Avillez, M. A. 2000, *MNRAS*, 315, 479
 de Avillez, M. A., & Breitschwerdt, D. 2004, *A&A*, 425, 899
 de Vaucouleurs, G. 1948, *Annales d'Astrophysique*, 11, 247
 Di Matteo, T., Croft, R. A. C., Springel, V., & Hernquist, L. 2003, *ApJ*, 593, 56
 Di Matteo, T., Springel, V., & Hernquist, L. 2005, *Nature*, 433, 604
 Dib, S., Bell, E., & Burkert, A. 2006, *ApJ*, 638, 797
 Dubinski, J., Mihos, J. C., & Hernquist, L. 1996, *ApJ*, 462, 576
 —. 1999, *ApJ*, 526, 607
 Dziourkevitch, N., Elstner, D., & Rüdiger, G. 2004, *A&A*, 423, L29
 Elmegreen, B. G., & Efremov, Y. N. 1997, *ApJ*, 480, 235
 Elmegreen, B. G., & Scalo, J. 2004, *ARA&A*, 42, 211
 Escala, A. 2006, *ArXiv Astrophysics e-prints*
 Fabian, A. C. 1999, *MNRAS*, 308, L39
 Ferrarese, L., Côté, P., Dalla Bontà, E., Peng, E. W., Merritt, D., Jordán, A., Blakeslee, J. P., Haşegan, M., Mei, S., Piatek, S., Tonry, J. L., & West, M. J. 2006, *ApJ*, 644, L21
 Ferrarese, L., & Ford, H. 2005, *Space Science Reviews*, 116, 523
 Ferrarese, L., & Merritt, D. 2000, *ApJ*, 539, L9
 Fujita, A., Martin, C. L., Mac Low, M., & Abel, T. 2003, *ApJ*, 599, 50
 Gebhardt, K., Bender, R., Bower, G., Dressler, A., Faber, S. M., Filippenko, A. V., Green, R., Grillmair, C., Ho, L. C., Kormendy, J., Lauer, T. R., Magorrian, J., Pinkney, J., Richstone, D., & Tremaine, S. 2000, *ApJ*, 539, L13
 Genzel, R., Eckart, A., Ott, T., & Eisenhauer, F. 1997, *MNRAS*, 291, 219
 Ghez, A. M., Duchêne, G., Matthews, K., Hornstein, S. D., Tanner, A., Larkin, J., Morris, M., Becklin, E. E., Salim, S., Kremenek, T., Thompson, D., Soifer, B. T., Neugebauer, G., & McLean, I. 2003, *ApJ*, 586, L127
 Ghez, A. M., Morris, M., Becklin, E. E., Tanner, A., & Kremenek, T. 2000, *Nature*, 407, 349
 Graham, A. W., Driver, S. P., Petrosian, V., Conselice, C. J., Bershady, M. A., Crawford, S. M., & Goto, T. 2005, *AJ*, 130, 1535
 Graham, A. W., Erwin, P., Caon, N., & Trujillo, I. 2001, *ApJ*, 563, L11
 Graham, A. W., & Guzmán, R. 2003, *AJ*, 125, 2936
 Graham, A. W. e. a. 2006, in preparation
 Haehnel, M. G., Natarajan, P., & Rees, M. J. 1998, *MNRAS*, 300, 817
 Haiman, Z., Ciotti, L., & Ostriker, J. P. 2004, *ApJ*, 606, 763
 Haiman, Z., & Quataert, E. 2004, *The Formation and Evolution of the First Massive Black Holes (ASSL Vol. 308: Supermassive Black Holes in the Distant Universe)*, 147–+
 Hernquist, L. 1989, *Nature*, 340, 687
 —. 1992, *ApJ*, 400, 460
 Ho, L. C. 1999, *ApJ*, 516, 672
 Hopkins, P. F., Hernquist, L., Cox, T. J., Di Matteo, T., Robertson, B., & Springel, V. 2006a, *ApJS*, 163, 1
 Hopkins, P. F., Hernquist, L., Cox, T. J., Robertson, B., Di Matteo, T., & Springel, V. 2006b, *ApJ*, 639, 700
 Hoyle, F., & Lyttleton, R. A. 1941, *MNRAS*, 101, 227
 Jappsen, A.-K., Klessen, R. S., Larson, R. B., Li, Y., & Mac Low, M.-M. 2005, *A&A*, 435, 611

- Kazantzidis, S., Mayer, L., Colpi, M., Madau, P., Debattista, V. P., Wadsley, J., Stadel, J., Quinn, T., & Moore, B. 2005, *ApJ*, 623, L67
- Kennicutt, Jr., R. C. 1998, *ApJ*, 498, 541
- King, A. 2003, *ApJ*, 596, L27
- Kormendy, J., & Richstone, D. 1995, *ARA&A*, 33, 581
- Kravtsov, A. V. 2003, *ApJ*, 590, L1
- Li, Y., Hernquist, L., Robertson, B., Cox, T. J., Hopkins, P. F., Springel, V., Gao, L., Di Matteo, T., Zentner, A. R., Jenkins, A., & Yoshida, N. 2006a, *ApJ*, submitted, astro-ph/0608190
- Li, Y., Mac Low, M.-M., & Klessen, R. S. 2004, *ApJ*, 614, L29
- . 2005a, *ApJ*, 620, L19
- . 2005b, *ApJ*, 626, 823
- . 2006b, *ApJ*, 639, 879
- Lotz, J. M., Miller, B. W., & Ferguson, H. C. 2004, *ApJ*, 613, 262
- Mac Low, M. 1999, *ApJ*, 524, 169
- Mac Low, M.-M., & Klessen, R. S. 2004, *Rev. Mod. Phys.*, 76, 125
- Macchetto, F., Marconi, A., Axon, D. J., Capetti, A., Sparks, W., & Crane, P. 1997, *ApJ*, 489, 579
- MacMillan, J. D., & Henriksen, R. N. 2002, *ApJ*, 569, 83
- Magorrian, J., Tremaine, S., Richstone, D., Bender, R., Bower, G., Dressler, A., Faber, S. M., Gebhardt, K., Green, R., Grillmair, C., Kormendy, J., & Lauer, T. 1998, *AJ*, 115, 2285
- Marconi, A., Axon, D. J., Macchetto, F. D., Capetti, A., Soarks, W. B., & Crane, P. 1997, *MNRAS*, 289, L21
- Marconi, A., & Hunt, L. K. 2003, *ApJ*, 589, L21
- Merritt, D., & Ferrarese, L. 2001, *ApJ*, 547, 140
- Mihos, J. C., & Hernquist, L. 1996, *ApJ*, 464, 641
- Miralda-Escudé, J., & Kollmeier, J. A. 2005, *ApJ*, 619, 30
- Mo, H. J., Mao, S., & White, S. D. M. 1998, *MNRAS*, 295, 319
- Monaco, P. 2004, *MNRAS*, 352, 181
- Murray, N., Quataert, E., & Thompson, T. A. 2005, *ApJ*, 618, 569
- Naab, T., & Burkert, A. 2003, *ApJ*, 597, 893
- Navarro, J. F., Frenk, C. S., & White, S. D. M. 1997, *ApJ*, 490, 493
- Nipoti, C., Londrillo, P., & Ciotti, L. 2003, *MNRAS*, 342, 501
- Rees, M. J. 1984, *ARA&A*, 22, 471
- Richstone, D., Ajhar, E. A., Bender, R., Bower, G., Dressler, A., Faber, S. M., Filippenko, A. V., Gebhardt, K., Green, R., Ho, L. C., Kormendy, J., Lauer, T. R., Magorrian, J., & Tremaine, S. 1998, *Nature*, 395, A14+
- Robertson, B., Cox, T. J., Hernquist, L., Franx, M., Hopkins, P. F., Martini, P., & Springel, V. 2006a, *ApJ*, 641, 21
- Robertson, B., Hernquist, L., Cox, T. J., Di Matteo, T., Hopkins, P. F., Martini, P., & Springel, V. 2006b, *ApJ*, 641, 90
- Rossa, J., van der Marel, R. P., Boeker, T., Gerssen, J., Ho, L. C., Rix, H.-W., Shields, J. C., & Walcher, C.-J. 2006, *ArXiv Astrophysics e-prints*
- Rownd, B. K., & Young, J. S. 1999, *AJ*, 118, 670
- Sazonov, S. Y., Ostriker, J. P., Ciotti, L., & Sunyaev, R. A. 2005, *MNRAS*, 358, 168
- Schödel, R., Ott, T., Genzel, R., Hofmann, R., Lehnert, M., Eckart, A., Mouawad, N., Alexander, T., Reid, M. J., Lenzen, R., Hartung, M., Lacombe, F., Rouan, D., Gendron, E., Rousset, G., Lagrange, A.-M., Brandner, W., Ageorges, N., Lidman, C., Moorwood, A. F. M., Spyromilio, J., Hubin, N., & Menten, K. M. 2002, *Nature*, 419, 694
- Sellwood, J. A., & Balbus, S. A. 1999, *ApJ*, 511, 660
- Sérsic, J. L. 1963, *Boletín de la Asociación Argentina de Astronomía La Plata Argentina*, 6, 41
- . 1968, *Atlas de galaxias australes (Cordoba, Argentina: Observatorio Astronomico)*, 1968)
- Shakura, N. I., & Sunyaev, R. A. 1973, *A&A*, 24, 337
- Silk, J., & Rees, M. J. 1998, *A&A*, 331, L1
- Springel, V. 2000, *MNRAS*, 312, 859
- Springel, V., Di Matteo, T., & Hernquist, L. 2005a, *ApJ*, 620, L79
- . 2005b, *MNRAS*, 361, 776
- Springel, V., & White, S. D. M. 1999, *MNRAS*, 307, 162
- Springel, V., Yoshida, N., & White, S. D. M. 2001, *New Astronomy*, 6, 79
- Steinmetz, M., & White, S. D. M. 1997, *MNRAS*, 288, 545
- Toomre, A., & Toomre, J. 1972, *ApJ*, 178, 623
- Tremaine, S., Gebhardt, K., Bender, R., Bower, G., Dressler, A., Faber, S. M., Filippenko, A. V., Green, R., Grillmair, C., Ho, L. C., Kormendy, J., Lauer, T. R., Magorrian, J., Pinkney, J., & Richstone, D. 2002, *ApJ*, 574, 740
- Walcher, C.-J., Boeker, T., Charlot, S., Ho, L. C., Rix, H.-W., Rossa, J., Shields, J. C., & van der Marel, R. P. 2006, *ArXiv Astrophysics e-prints*
- Walcher, C. J., van der Marel, R. P., McLaughlin, D., Rix, H.-W., Böker, T., Häring, N., Ho, L. C., Sarzi, M., & Shields, J. C. 2005, *ApJ*, 618, 237
- Wehner, E. H., & Harris, W. E. 2006, *ApJ*, 644, L17
- Whitworth, A. P. 1998, *MNRAS*, 296, 442
- Wong, T., & Blitz, L. 2002, *ApJ*, 569, 157
- Wood, K., & Loeb, A. 2000, *ApJ*, 545, 86
- Wyithe, J. S. B., & Loeb, A. 2003, *ApJ*, 595, 614
- . 2005, *ApJ*, 634, 910